Phenology-Climate Dynamics in Response to Changes in Land and Water Use Practices in Central Asia

Introduction

Central Asia includes five countries: Kazakhstan, Kyrgyzstan, Tajikistan, Turkmenistan, and Uzbekistan (Figure 1). The Central Asia region lies in the middle of the Eurasian continent, covering approximately four million square km (Gleason 1997).

Figure 1: Central Asia

Agriculture is the key industry of the region (Saiko and Zonn 2000) and due to that its main environmental issues are associated with limited water availability throughout most of the

territory. With socio-economic and political changes followed the USSR collapse in 1991, water resources became one of the most important natural resources in the region (Glantz 2005; Elhance 1997).

During the Soviet period, from the 1930s to the late 1990s, agriculture in the region was developing in the direction of irrigated expansion (Saiko and Zonn 2000). From the 1970s the rate of agricultural growth was especially fast, leading to a 70% increase in area of irrigated lands for the entire region (Saiko and Zonn 2000). Such agricultural policies have influenced the long-term landscape dynamics causing ecological issues in the Central Asia region (Saiko and Zonn 2000; Elhance 1997). One of the examples of the regional environmental problems is the desiccation of the Aral Sea. One of the major water contributors to the Aral Sea is the Amu Darya - a transboundary river between Turkmenistan and Uzbekistan (Figure 1). The river is one of the largest fresh water sources in Central Asia and the main irrigation source for Turkmenistan (Hanmamedov and Rejepov 2007). Due to the specifics of the poor and sandy soil and dry continental climatic conditions of Turkmenistan and Uzbekistan the growth of any crops in these arid environments requires irrigation during most of the vegetative period. The Karakum canal in Turkmenistan is one of the largest water canals in the world (over 1300 km: Figure 1), uses about one quarter of the water from the Amu Darya to open up large areas of land to agriculture (Carlisle 1997; Glantz 2005). Almost half of the canal water volume is lost through evaporation and infiltration causing an intense soil salinization from water evaporation and ineffective leaching of soils (O'Hara 1997; Waltham and Sholji 2001; Saiko and Zonn 2000). In light of recent geopolitical and economic changes along with intense land conversion in Central Asia prior to and after the Soviet Union collapse, there is a pressing need to develop new monitoring

and management efforts that aim to address landscape change patterns as well as their socio-economic implications for the region.

Methods

Goals and Objectives

The goal of this research is to evaluate landscape change dynamics in response to climate variability trends and altered patterns in land use practices and water resources allocation as a result of socio-economic and political changes in Central Asia. The research aimed to characterize the extent to which bioclimatic drivers and land use patterns impact spatio-temporal trends in land surface phenology. This project sought to investigate change patterns in terrestrial phenology and long-term climate variability in Central Asia by differentiating human-driven change phenology responses. Land surface vegetation phenology (spatio-temporal patterns in vegetation growth dynamics) was used as an approach to evaluate landscape changes.

Interannual land surface phenology dynamics are used as a proxy for the assessment of vegetation response to water availability and redistribution due to changed land use patterns. To be able to assess landscape changes and their socio-economic implications for the Central Asian ecosystems, long term (1981-2006) time series of remotely sensed vegetation greenness data are used to characterize interannual vegetation phenological responses. Additionally, regional scale climate patterns (precipitation, temperature) were examined to separate human-induced effects in land surface phenology from those that are driven by long term climate variability effects. All the analyses for this part of the research were performed on a regional extent of Turkmenistan and Uzbekistan.

Study Sites

Representative study sites were chosen to assess changes in land cover through vegetation response due to altered patterns of water resources allocation. The focus areas for this research are the zones near the Amu Darya and Karakum canal. Because these two water bodies are located mostly within Turkmenistan and Uzbekistan and are crucial for their economies, the extent of the countries is considered a study site (Figure 2). The two countries are about the same size in terms of land area (Turkmenistan: 488,100 km^2; Uzbekistan: 477,000 km^2) and have similar physiographic conditions: ranging from the flat desert terrain that comprises about 80% of their territories to mountainous landscapes.

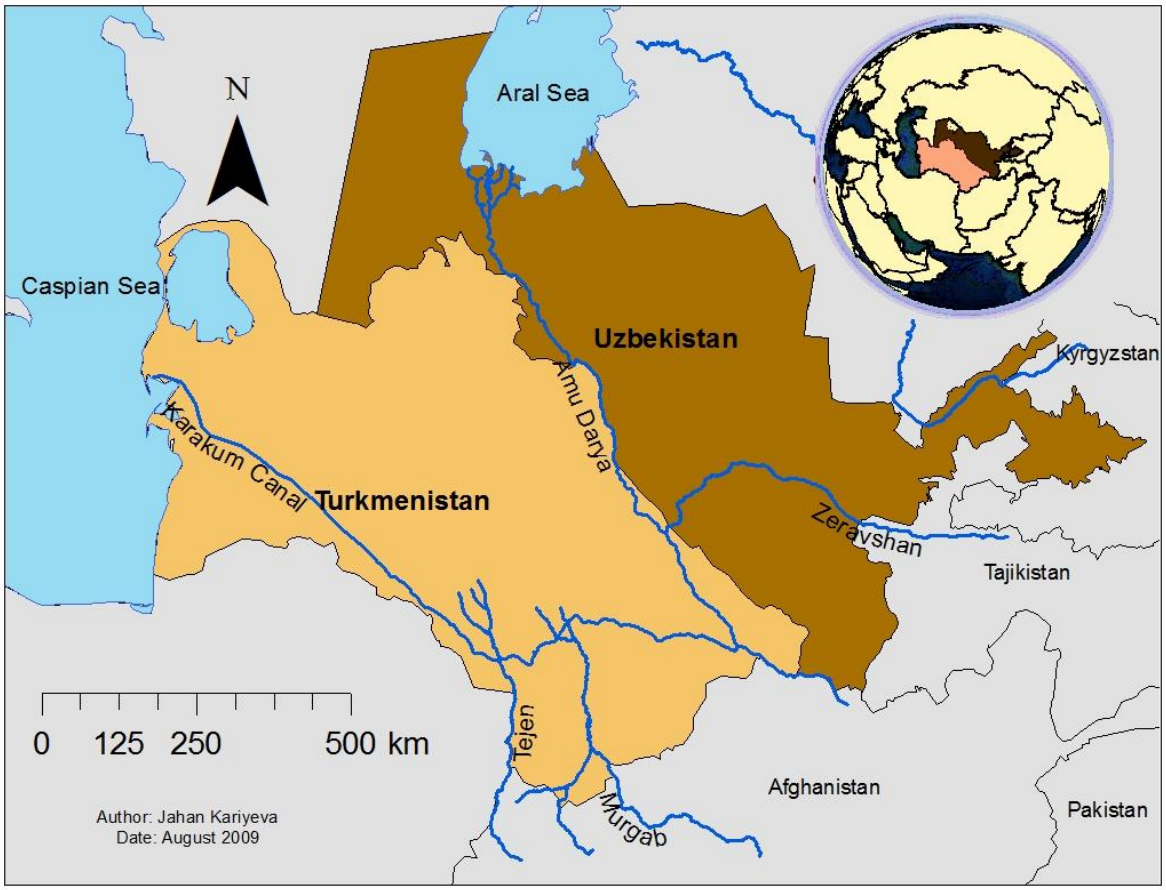

Figure 2: Study site extent: Turkmenistan and Uzbekistan and zones of influence of the Amu Darya and Karakum canal

Datasets

Datasets that were used for the study were readily available for the entire study site (Turkmenistan and Uzbekistan) and were preprocessed into separate raster format images with particular type of data. *Vegetation greenness and productivity data*: long-term (1981-2006) time-series of vegetation greenness datasets are used to assess vegetation productivity and quantify phenology for sites in Uzbekistan and Turkmenistan. The datasets are bi-weekly composite periods of Normalized Difference Vegetation Index (NDVI; 8 km) time-series data of the Global Inventory Modeling and Mapping Studies (GIMMS) data obtained from a series (7, 9, 11, 14, 16 and 17) of Advanced Very High Resolution Radiometer (AVHRR) platforms (Tucker et al. 2005). The advantage of this bi-weekly dataset is its 26-year temporal extent that allowing detection and characterization of the trends and anomalies in vegetation variability during the study period. *Climate data:* gridded Climate Research Unit (CRU) datasets from Consultative Group on International Agricultural Research Consortium for Spatial Information (CGIAR-CSI) and British Atmospheric Data Centre (BADC) for 26 years (1981-2006) were used as the climate datasets to assess weather patterns for the Turkmenistan-Uzbekistan study site extent (CGIAR-CSI 2006). This monthly composite period dataset with 0.5 degree cell resolution includes the following climate characteristics: precipitation, average temperature, max temperature, min temperature, vapor pressure, and derived vapor pressure deficit datasets. However, for this part of the analysis only precipitation and temperature variables were used. *Land use/management records and datasets:* Datasets identifying irrigated agriculture areas in Turkmenistan-Uzbekistan study site were obtained from the International Water Management Institute's (IWMI) Global Irrigated Area Map (GIAM) dataset (Thenkabail et al. 2008; Thenkabail et al. 2006).

Data Analysis

The initial step of the project was to derive phenological metrics (pheno-metrics). "TIMESAT" time-series analysis software will be used to create eleven phenological metrics that included dates of the growing season, such as start, peak, end, and duration, and corresponding vegetation greenness values, among others (Jönsson and Eklundh 2004, 2002). Eleven phenological were created for each calendar year within the 26-year temporal extent of observed NDVI records (Figure 2 and Table 1). Figure 3 demonstrates an example of one of the derived metrics: start of growing season date for 1991. The scale of the image represents calendar months.

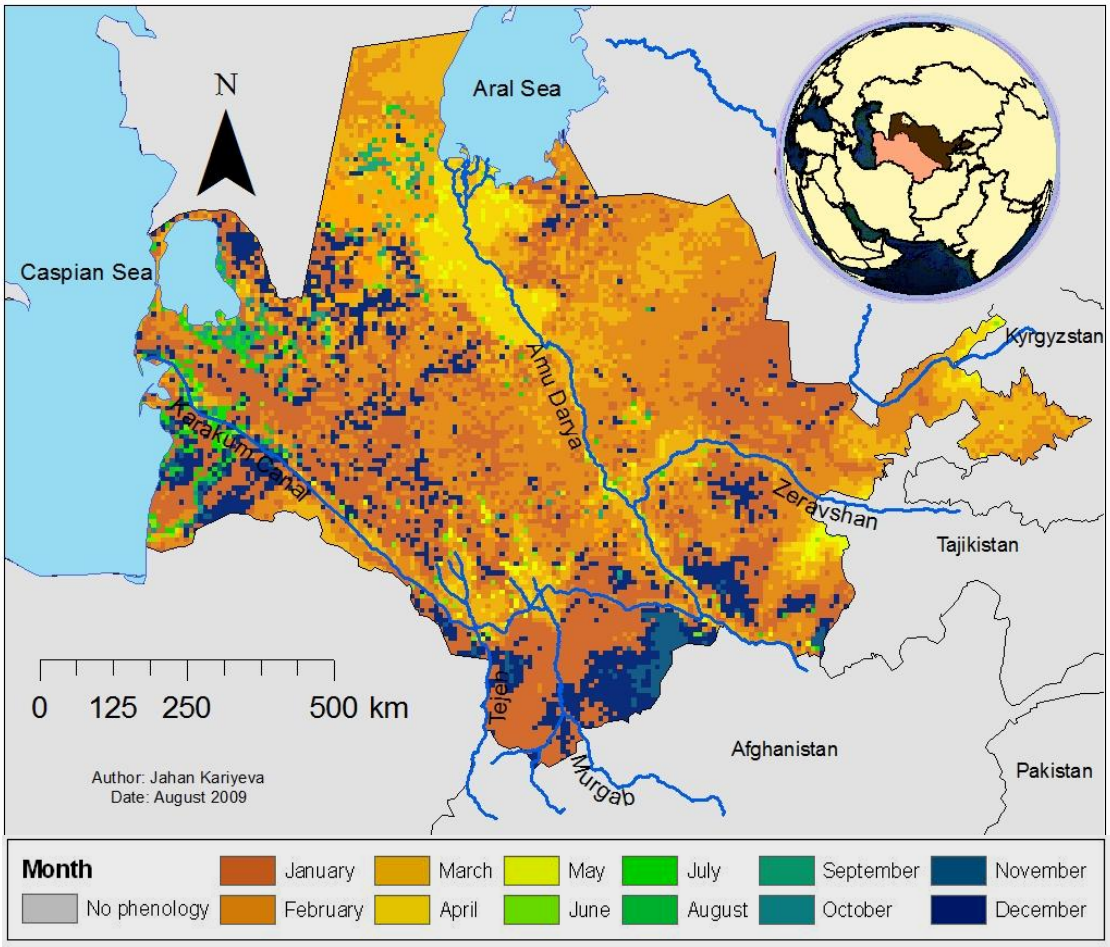

Figure 3: Example of spatially explicit phenological metric: start of growing season for 1991

Table 1: List of derived phenological metrics

Timing phenological metrics	Greenness phenological metrics
Start of the growing season (SOS)	Rate of greenup (Left derivative: LD)
Middle of the growing season (POS)	Rate of senescence (Right derivative: RD)
End of the growing season (EOS)	Base NDVI greenness (Base value: BS)
Length of the growing season (LOS)	Peak NDVI greenness (Peak value: PK)
	Greenness amplitude (Amplitude: AMP)
	Seasonal greenness (Small integrated value: SI)
	Seasonal biomass (Large integrated value: LI)

Next step was to create seasonal climate metrics (precipitation and temperature) from the monthly composite periods. There were four seasonal periods were created for the climate metrics. Winter seasons include November, December, January, and February (NDJF) months. Spring seasons include February, March, April, and May (FMAM) months. Summer seasons consist of May, June, July, and August (MJJA) month. Fall includes of August, September, October, and November (ASON) months. Figure 4 shows an example of one of the seasonal climate metrics: spring temperature for 1991. For the temperature metrics values were averaged for four months representing the season, while precipitation values were summed for those four months.

Table 2: List of seasonal climate metrics

Precipitation	Temperature
Accumulated winter precipitation (NDJF)	Average winter precipitation (NDJF)
Accumulated spring precipitation (FMAM)	Average spring precipitation (FMAM)
Accumulated summer precipitation (MJJA)	Average summer precipitation (MJJA)
Accumulated fall precipitation (ASON)	Average fall precipitation (ASON)

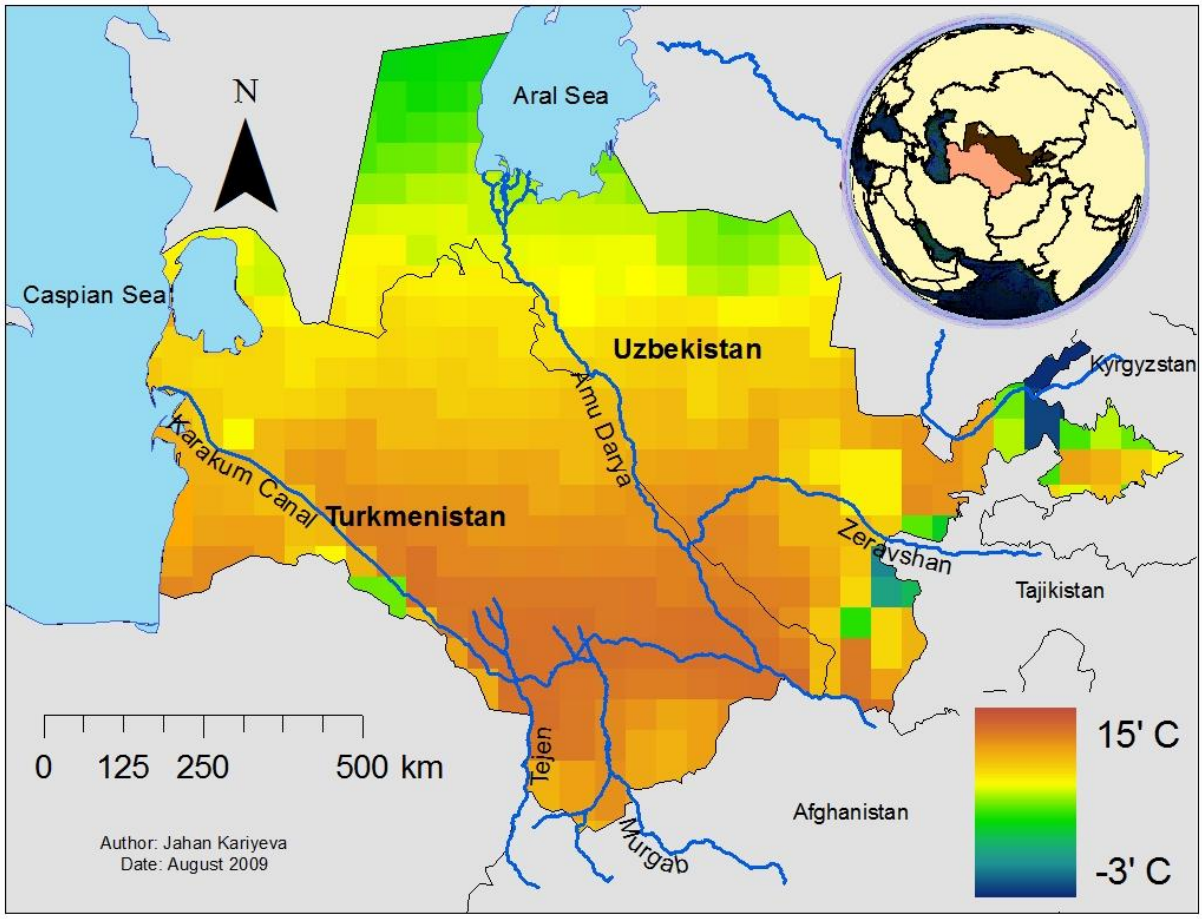

Figure 4: Example of seasonal climate metric: spring temperature for 1991

Next step was to perform standardized covariance analysis to be able to determine whether and how phenology is associated with climate. Standardized covariance is also known as Pearson's correlation coefficient (*r*), values of which lie in the range from -1 to +1 and provide a standardized measure of the linear association between two variables, i.e. in this case measure of the strength of the linear association between phenology and climate variables. In order to derive the correlation coefficient at pixel per pixel basis, both datasets had to pre-processed: projected into the same projection, sized into the same pixel resolution, had to have the same temporal extent, and clipped to the same spatial extent (Figure 3-4). Therefore, time

series of thirteen phenological (Table 1) and eight seasonal climate metrics (Table 2) were correlated to each other over a 26-year period (1981-2006). To create output images only those correlation coefficient (*r*) values that had 90% probability were accepted. Furthermore, all the accepted *r* values were reclassified into three classes (Table 3).

Table 3: List of reclassified correlation coefficient values with 90% probability

Old *r* values	**New *r* values**
(-1.0) – (-0.6)	High negative correlation
(-0.6) – (-0.3)	Medium negative correlation
(-0.3) – (-0.1)	Low negative correlation
(-0.1) – 0.1	No correlation
0.1 – 0.3	Low positive correlation
0.3 – 0.6	Medium positive correlation
0.6 – 1.0	High positive correlation

One of the steps of this analysis was to summarize obtained measures of linear strength between phenology and climate dynamics by differentiating human-induced from climatic drivers. Anthropogenic impact was based on a dataset with land use classes that were created from the IWMI GIAM irrigated agriculture datasets (Thenkabail et al. 2008; Thenkabail et al. 2006) for the Turkmenistan-Uzbekistan study site (Figure 1). Finally, derived imagery outputs with *r* values that demonstrated 90% probability were classified by two land cover classes: agriculture (AG) and non-agriculture (NAG).

Results and Conclusions

Generally phenological metrics demonstrated positive correlations to precipitation and negative correlations to temperature. For the purpose of this report only results obtained for timing phenological metrics will be displayed and discussed in a detailed manner: start of

growing season (SOS) in Figure 5; middle of growing season (POS) in Figure 6; end of growing season (EOS) in Figure 7. Due to the limited space of the report those three abovementioned timing metrics (SOS, POS, and EOS) will be discussed with their association to spring temperature only.

An earlier start of season was associated with increasing spring temperatures for pixels in agricultural and riparian areas and for pixels in non-agricultural areas an earlier start of season was correlated to lower spring temperatures (Figure 5). Peak of growing season demonstrated to have earlier dates with lower spring temperatures for pixels in both agriculture and non-agriculture land cover types (Figure 6). End of the growing season revealed interesting results, showing that an earlier end of season was correlated with increasing spring temperatures for pixels in the agricultural and riparian areas of Amu Darya, Karakum canal, and Zeravshan River (Uzbekistan), while pixels for non-agricultural sites have shown to have later end of season dates with increasing spring temperature in Turkmenistan and earlier dates in Uzbekistan (Figure 7).

Arid and semi-arid Central Asian ecosystems are exposed to complex climate variations and economic transitions followed the USSR collapse in 1991. Dynamics of land surface phenology are interrelated to climatic and socio-economic variations. Study results demonstrate that satellite-based phenology analysis can be used to characterize landscape-scale change dynamics in light of climate variability and land use changes in Central Asia. The phenological metrics demonstrated to be related to climate metrics as well as to different land use patterns (agriculture and non-agriculture). Therefore, application of phenological metrics can be helpful in improving land cover classifications over seasons.

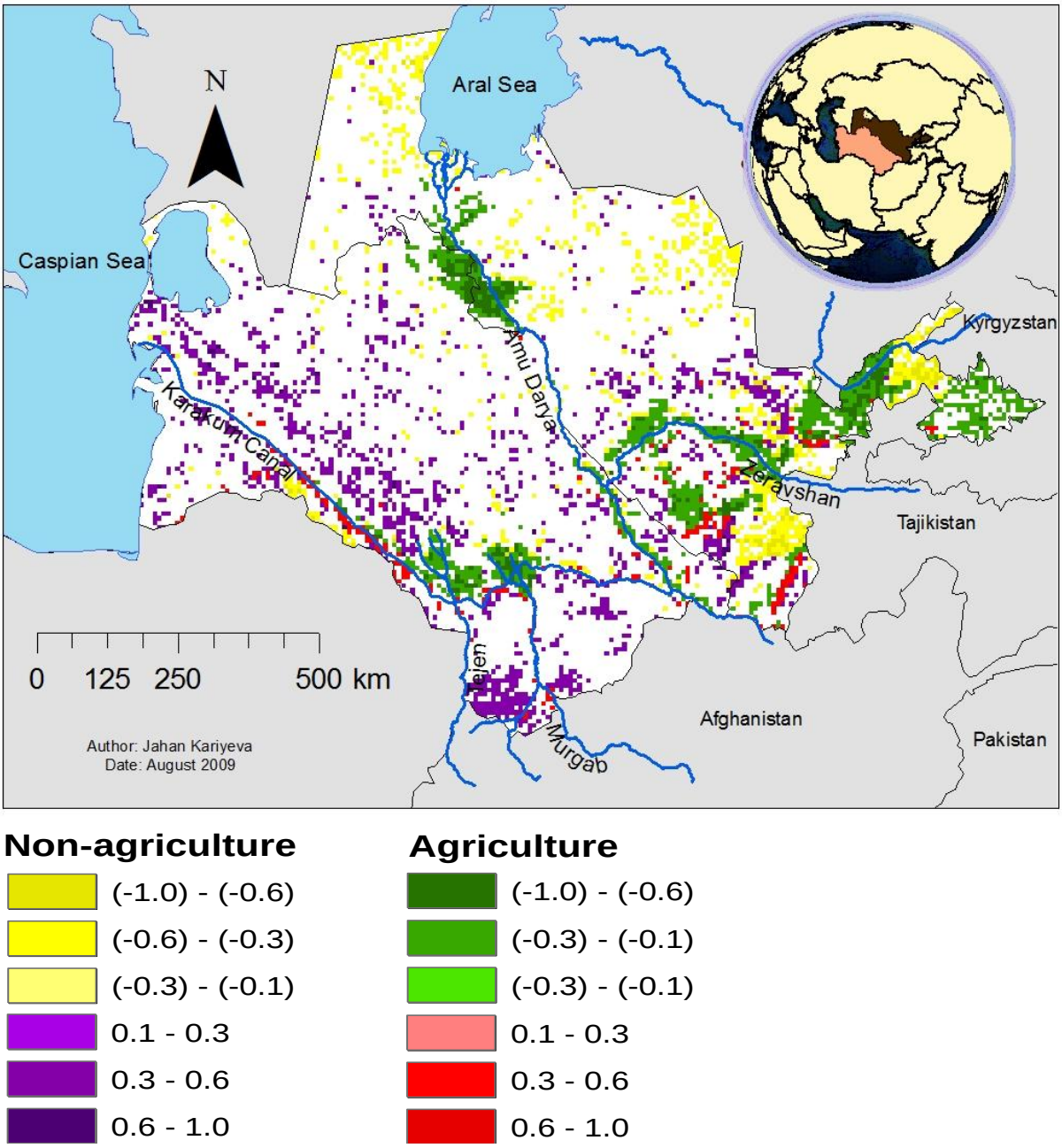

Non-agriculture	Agriculture
(-1.0) - (-0.6)	(-1.0) - (-0.6)
(-0.6) - (-0.3)	(-0.3) - (-0.1)
(-0.3) - (-0.1)	(-0.3) - (-0.1)
0.1 - 0.3	0.1 - 0.3
0.3 - 0.6	0.3 - 0.6
0.6 - 1.0	0.6 - 1.0

Figure 5: Strength of linear relationship (correlation coefficient (*r*) with 90% probability) between Start of Growing Season (SOS) and Average Spring Temperature

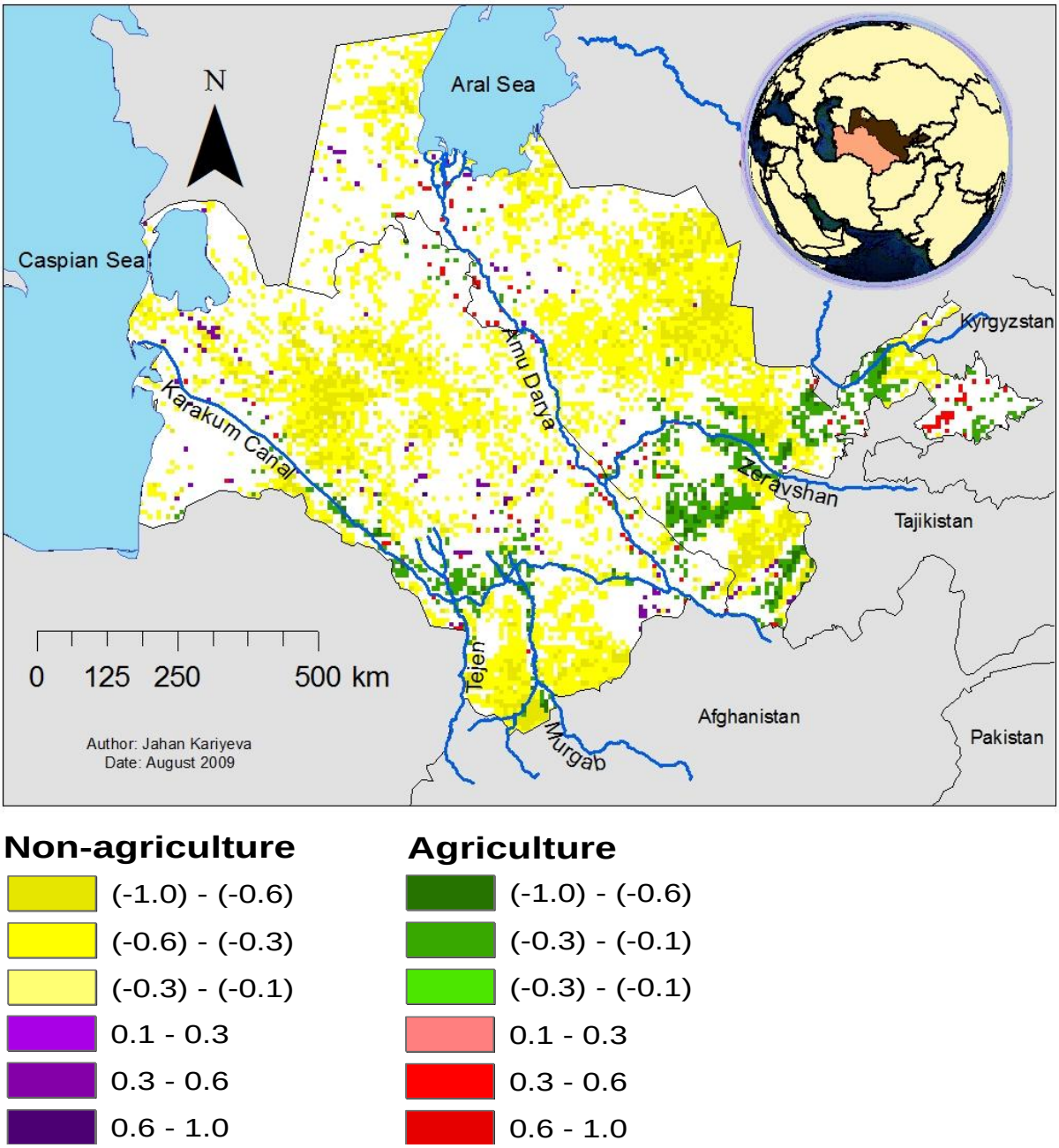

Non-agriculture

- (-1.0) - (-0.6)
- (-0.6) - (-0.3)
- (-0.3) - (-0.1)
- 0.1 - 0.3
- 0.3 - 0.6
- 0.6 - 1.0

Agriculture

- (-1.0) - (-0.6)
- (-0.3) - (-0.1)
- (-0.3) - (-0.1)
- 0.1 - 0.3
- 0.3 - 0.6
- 0.6 - 1.0

Figure 6: Strength of linear relationship (correlation coefficient (*r*) with 90% probability) between Middle of Growing Season (POS) and Average Spring Temperature

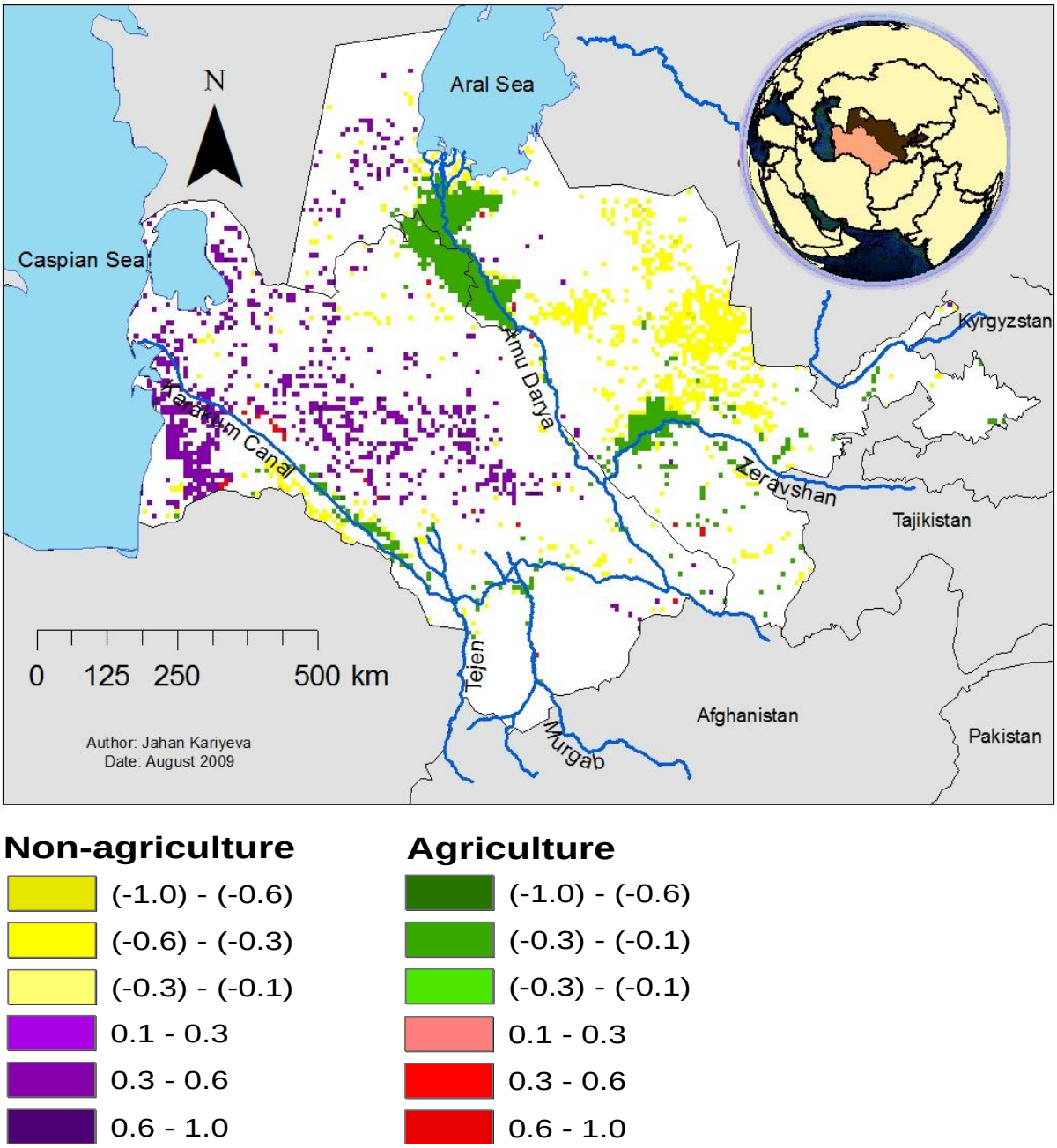

Non-agriculture	Agriculture
(-1.0) - (-0.6)	(-1.0) - (-0.6)
(-0.6) - (-0.3)	(-0.3) - (-0.1)
(-0.3) - (-0.1)	(-0.3) - (-0.1)
0.1 - 0.3	0.1 - 0.3
0.3 - 0.6	0.3 - 0.6
0.6 - 1.0	0.6 - 1.0

Figure 7: Strength of linear relationship (correlation coefficient (*r*) with 90% probability) between End of Growing Season (EOS) and Average Spring Temperature

Reference:

Carlisle, H. L. 1997. Hydropolitics in Post-Soviet Central Asia: International Environmental Institutions and Water Resource Control. In *The Political Economy of International Environmental Cooperation*. Santa Cruz, California: University of California Institute on Global Conflict and Cooperation.

CGIAR-CSI. 2006. CGIAR-CSI Climate Research Unit (CRU) TS 2.1 Database: Consultative Group on International Agricultural Research Consortium for Spatial Information: http://csi.cgiar.org

Elhance, A. P. 1997. Conflict and cooperation over water in the Aral Sea basin. *Studies in Conflict & Terrorism* 20 (2):207-218.

Glantz, M. H. 2005. Water, Climate, and Development Issues in the Amu Darya Basin. *Mitigation and Adaptation Strategies for Global Change* 10 (1):23-50.

Gleason, G. 1997. *The Central Asian States: Discovering Independence, Westview series on the post-Soviet republics*. Boulder, Colo.: Westview Press.

Hanmamedov, M. A., and O. R. Rejepov. 2007. О Рациональном Использовании Водных Ресурсов Туркменистана (Rational Water Use in Turkmenistan). *Проблемы Освоения Пустынь (Problems of Deserts Development)* 1:26-27.

Jönsson, P., and L. Eklundh. 2002. Seasonality extraction by function fitting to time-series of satellite sensor data. *Geoscience and Remote Sensing, IEEE Transactions on* 40 (8):1824-1832.

———. 2004. TIMESAT - a program for analyzing time-series of satellite sensor data. *Computers & Geosciences* 30 (8):833-845

O'Hara, S. L. 1997. Irrigation and land degradation: implications for agriculture in Turkmenistan, central Asia. *Journal of Arid Environments* 37 (1):165-179.

Saiko, T. A., and I. S. Zonn. 2000. Irrigation expansion and dynamics of desertification in the Circum-Aral region of Central Asia. *Applied Geography* 20 (4):349-367.

Thenkabail, P. S., Biradar C.M., P. Noojipady, V. Dheeravath, Y. J. Li, M. Velpuri, M. Gumma, G. P. O. Reddy, H. Turral, X. L. Cai, J. Vithanage, M. Schull, and R. Dutta. 2008. Global Irrigated Area Map (GIAM) for the End of the Last Millennium Derived from Remote Sensing. *International Journal of Remote Sensing (accepted, in press)*.

Thenkabail, P. S., C. M. Biradar, H. Turral, P. Noojipady, Y. J. Li, J. Vithanage, V. Dheeravath, M. Velpuri, Schull M., X. L. Cai, and R. Dutta. 2006. An Irrigated Area Map of the World (1999) derived from Remote Sensing. In *Research Report # 105*, 74: International Water Management Institute.

Tucker, C. J., J. E. Pinzon, M. E. Brown, D. A. Slayback, E. W. Pak, R. Mahoney, E. F. Vermote, and N. E. Saleous. 2005. An extended AVHRR 8-km NDVI dataset compatible with MODIS and SPOT vegetation NDVI data. *International Journal of Remote Sensing* 26 (20):4485 - 4498.

Waltham, T., and I. Sholji. 2001. The demise of the Aral Sea - an environmental disaster. *Geology Today* 17 (6):218-228.